EPJ Web of Conferences **101**, 05008 (2015)
DOI: 10.1051/epjconf/201510105008

Nonadiabatic analysis of rosette modes of oscillations in rotating stars and their contribution to angular momentum transport

Masao Takata[1,a] and Hideyuki Saio[2]

[1] Department of Astronomy, School of Science, The University of Tokyo, 7-3-1 Hongo, Bunkyo-ku, Tokyo 113-0033, Japan
[2] Astronomical Institute, Graduate School of Science, Tohoku University, 6-3 Aramaki, Aoba-ku, Sendai 980-8578, Japan

Abstract. Rosette modes compose a peculiar group of oscillation modes in rotating stars. Although they have been investigated in some theoretical works, it has not been clear yet whether these modes are excited in real stars or not. In order to study this problem, a stability analysis of the modes is performed. It turns out that some rosette modes are unstable due to the kappa mechanism in a model of slowly pulsating B stars. It is also examined how unstable rosette modes can transport angular momentum in stars.

1 Introduction

Rosette modes are a class of eigenmodes of oscillations that are found in rotating stars. Their frequencies are in the range of gravity modes, but not below twice the rotation frequency, the domain in which the Coriolis force plays a dominant role in the oscillation motion. The most remarkable characteristic of the modes appears in the structure of the eigenfunctions. The kinetic energy of the oscillation distributes along rosette patterns on the meridional plane. This is the reason why the modes have their name. The modes have been discovered recently by accident [1] in numerical computations of oscillation modes of uniformly rotating polytropic models, when physical properties of gravito-inertial modes in rapidly rotating stars are studied [2].

The mechanism to form the rosette modes has been analysed based on a perturbation theory [3], assuming that rotation is slow (and uniform). The key point is considerable interaction caused by the second-order effect of the Coriolis force among multiple eigenmodes that have almost the same frequencies (close degeneracy) in the non-rotating limit. The possibility of such (close) degeneracy has already been recognised before in the perturbative treatment of the effect of rotation on stellar oscillations [e.g. 4]. However, a primary stress has usually been put on the case of two degenerate modes, whereas it is essential for the rosette modes to consider close degeneracy among many eigenmodes.

The properties of the rosette modes have been further studied. Although the modes have originally been found among axisymmetric modes, it has been shown that non-axisymmetric rosette modes can also be formed [5]. A detailed analysis has clarified that retrograde modes tend to have clearer rosette patterns than prograde modes. Moreover, the rosette patterns of the modes have been successfully described by simple relations that are derived based on an asymptotic analysis [6].

This paper presents two more steps of our analysis of the rosette modes. We first examine in section 2 whether the modes can be excited in real stars or not. We perform a linear stability analysis of the rosette modes of an early-type zero-age main sequence (ZAMS) stellar model based on the nonadiabatic calculation. Secondly, we evaluate in section 3 the contribution of the modes to the transport of angular momentum inside the model. A summary is finally given in section 4.

[a] e-mail: takata@astron.s.u-tokyo.ac.jp

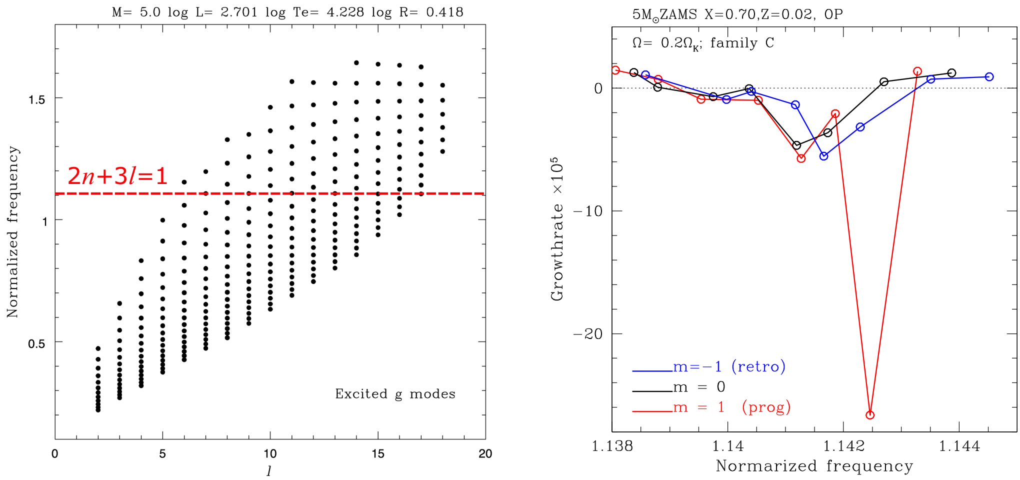

Fig. 1. Left panel: plot of the real part of the eigenfrequency of unstable gravity modes (without rotation) versus the spherical degree, l, of a $5\,M_\odot$ ZAMS stellar model with the hydrogen mass fraction of $X = 0.70$ and the heavy-element mass fraction of $Z = 0.02$. The eigenfrequency is normalised by $\left(GM/R^3\right)^{1/2}$. Here, G is the gravitational constant, while M and R mean the mass and the radius of the model, respectively. The red dashed horizontal line indicates a family of modes that have almost the same frequencies. **Right panel**: growth rate of the rosette modes that come from the family of close degeneracy in the left panel as functions of the real part of the normalised eigenfrequency. The rotation rate, Ω, is assumed to be 20 % of the Keplerian rotation rate, Ω_{K}, at the equator. The positive (negative) values of the growth rate mean that the corresponding modes are unstable (stable). The lines with different colours indicate different values of the azimuthal order, m.

2 Stability analysis of rosette modes of an early-type ZAMS stellar model

In order to discuss whether the rosette modes can be excited in real stars or not, we examine the stability of oscillation modes of a $5\,M_\odot$ ZAMS model, which can be regarded as a representative model of slowly pulsating B stars [7, 8].

It is first confirmed in the case of no rotation that many high-degree gravity modes are destabilised by the iron opacity bump that is located at the temperature of about 2×10^5 K. Note that we have used the OP opacity [9] in this calculation. The left panel of figure 1 shows the plot of the real part of the eigenfrequency of the unstable modes versus the spherical degree, l. Among those unstable modes, we can identify a family of close degeneracy that is designated by the horizontal dashed line. This family is specified by a relation of $2n + 3l = 1$, where n is the radial order. Although l of the unstable modes is limited to all the odd numbers between 7 and 17, we may regard that some stable modes with $l \leq 5$ and $l \geq 19$ also belong to the family. We concentrate on rosette modes that originate from this particular family. Examples of the (adiabatic) rosette modes are shown in figure 2 for the rotation rate, Ω, of 20 % of the Keplerian rotation rate, Ω_{K}, at the equator.

We then use the program developed by [10] to calculate nonadiabatic rosette modes. It is found that some of the rosette modes are actually unstable if the rotation rate satisfies $\Omega \lesssim 0.25\Omega_{\mathrm{K}}$. (The upper limit corresponds to the equatorial rotation velocity of about 150 km s^{-1}.) The right panel of figure 1 shows the growth rate of rosette modes as functions of the frequency. Corresponding to the fact that the eigenfunctions of rosette modes can generally be expressed as linear combinations of eigenfunctions in the case of no rotation, we can understand the stability property of the rosette modes based on that of their constituent modes in the non-rotating limit. In fact, only those rosette modes that have significant contribution from unstable modes (shown in the left panel of figure 1) tend to be excited. For example, the highly-stable prograde rosette mode with the normalised frequency of about 1.1425 in the right panel of figure 1 suffers from severe radiative damping caused by some exceptionally high-degree components. Similarly, as the rotation rate is higher, more modes, particularly those with higher degrees, are involved in the rosette modes because of stronger interaction caused by the Coriolis force. This results in the larger damping effect and eventually stabilises all of the rosette modes.

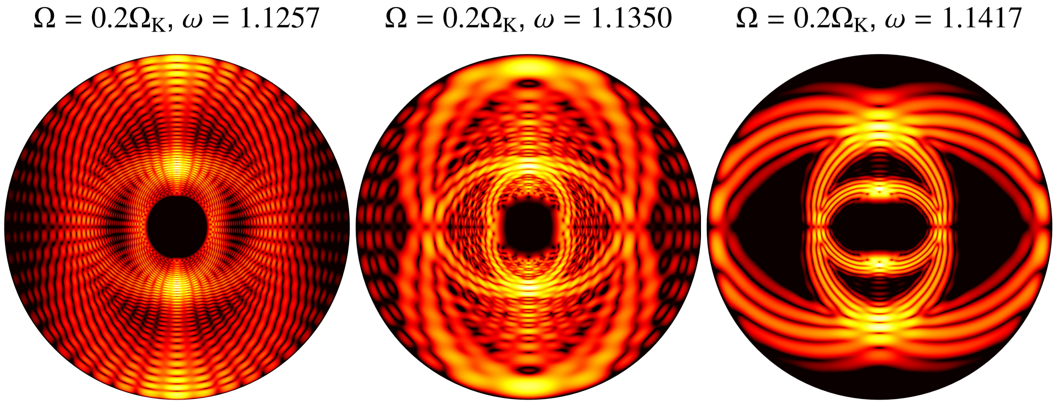

Fig. 2. Examples of rosette modes of the 5 $M_\odot$ZAMS model that come from the family of close degeneracy in the left panel of figure 1. Plotted is the distribution of the kinetic energy density carried by the meridional component of the displacement vector on the meridional plane, multiplied by the square of the distance from the centre for visibility. The results have been obtained by purely adiabatic computation for retrograde modes with the azimuthal order of -1. The rotation rate is assumed to be 20 % of the Keplerian rotation rate at the equator. The normalised frequency, ω, of each mode is shown above each panel.

3 Angular momentum transport

An interesting topic related to unstable oscillation modes is their transport of angular momentum in stars. We examine how the rosette modes can contribute to the transport.

Following [11], we adopt the Lagrangian description of wave-mean flow interactions, which has been developed in meteorology [e.g. 12]. We particularly use equation (A28) of [11], which is given by

$$\rho \frac{d\langle h \rangle}{dt} = -\nabla \cdot \langle \boldsymbol{F} \rangle \ , \tag{1}$$

with $\boldsymbol{F}$ defined by

$$\boldsymbol{F} = \frac{\partial p'}{\partial \phi} \boldsymbol{\xi} + \frac{\partial \Phi'}{\partial \phi} \left(\rho \boldsymbol{\xi} + \frac{\nabla \Phi'}{4\pi G} \right) . \tag{2}$$

The meanings of the symbols in equations (1) and (2) are as follows: ρ is the density of the equilibrium structure; d/dt the Lagrangian time derivative (for a fixed mass element); $\langle\rangle$ the Lagrangian mean over the azimuthal angle; h the specific angular momentum around the rotation axis; ϕ the azimuthal angle; $\boldsymbol{\xi}$, p' and Φ' are the (complex) eigenfunctions of nonadiabatic stellar oscillations, which represent the displacement vector, the Eulerian perturbation to the pressure and the Eulerian perturbation to the gravitational potential, respectively. As discussed in [11], the integral of the right-hand side of equation (1) over the whole solid angle is closely related to the derivative of the work function of the stability analysis, which is positive (negative) in the region of excitation (damping). In fact, equation (1) essentially describes the physical picture that angular momentum is given to (taken from) the equilibrium structure by waves that compose the oscillation modes at the places where prograde modes are damped (excited). (The situation is opposite for retrograde modes, because $\boldsymbol{F}$ is proportional to the azimuthal order, m.)

We evaluate the right-hand side of equation (1) for a retrograde rosette mode with $m = -1$ that has been computed in section 2. While the distribution of the kinetic energy density is close to that shown in the rightmost panel of figure 2, the normalised distribution of $-\nabla \cdot \langle \boldsymbol{F} \rangle$ is presented in figure 3. It is clear that the distribution preserves the rosette structure that changes significantly as a function of the latitude. This suggests that unstable rosette modes might uniquely contribute to the angular momentum transport in the latitudinal direction. On the other hand, we have also calculated the integral of $-\nabla \cdot \langle \boldsymbol{F} \rangle$ over the whole solid angle. The comparison of the result to that of an ordinary (non-rosette) mode with a similar frequency shows no considerable difference. It is generally observed in the angle-integrated

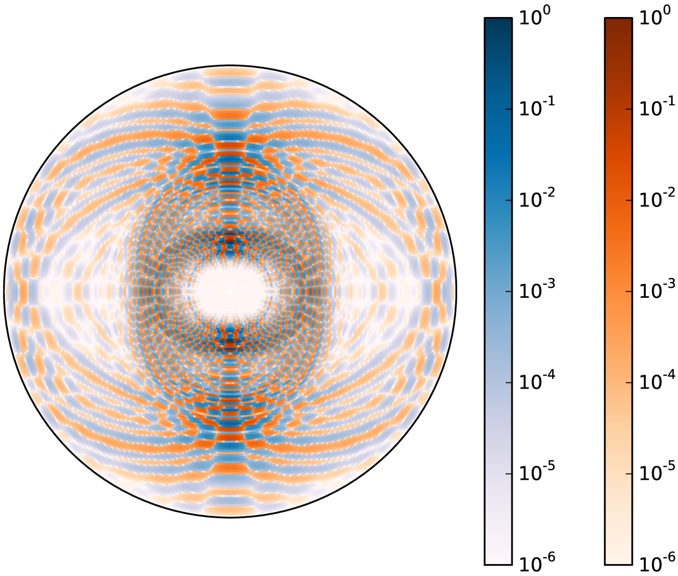

Fig. 3. The contribution of a retrograde rosette mode to the change of specific angular momentum at each point on the meridional plane. The mode has almost the same structure as an adiabatic mode that is shown in the rightmost panel of figure 2. The computation has been done based on the right-hand side of equation (1). The blue (red) regions indicate the places of positive (negative) values.

distribution that large contribution is found only near the ionisation region of iron-peak elements, which is close to the surface.

4 Summary

A nonadiabatic analysis of rosette modes of a $5\,M_\odot$ ZAMS stellar model has been performed. It is found that some rosette modes are destabilised by the standard kappa mechanism of iron-peak elements. The contribution of those modes to the transport of angular momentum has been examined. It is argued that rosette modes might provide a unique channel of angular momentum transport particularly in the latitudinal direction.

This work was partially supported by JSPS KAKENHI Grant Number 26400219.

References

1. J. Ballot, F. Lignières, V. Prat, D.R. Reese, M. Rieutord, *2D computations of g modes*, in *Progress in Solar/Stellar Physics with Helio- and Asteroseismology*, edited by H. Shibahashi, M. Takata, A. E. Lynas-Gray (Astronomical Society of the Pacific, San Francisco, 2012), Vol. 462 of *ASP Conference Series*, pp. 389–397
2. J. Ballot, F. Lignières, D.R. Reese, M. Rieutord, A&A **518**, A30 (2010)
3. M. Takata, H. Saio, PASJ **65**, 68 (2013)
4. W.A. Dziembowski, P.R. Goode, ApJ **394**, 670 (1992)
5. H. Saio, M. Takata, PASJ **66**, 58 (2014)
6. M. Takata, PASJ **66**, 80 (2014)
7. A. Gautschy, H. Saio, MNRAS **262**, 213 (1993)
8. W.A. Dziembowski, P. Moskalik, A.A. Pamyatnykh, MNRAS **265**, 588 (1993)
9. N.R. Badnell, M.A. Bautista, K. Butler, F. Delahaye, C. Mendoza, P. Palmeri, C.J. Zeippen, M.J. Seaton, MNRAS **360**, 458 (2005)
10. U. Lee, I. Baraffe, A&A **301**, 419 (1995)
11. U. Lee, PASJ **65**, 122 (2013)
12. R. Grimshaw, Annual Review of Fluid Mechanics **16**, 11 (1984)